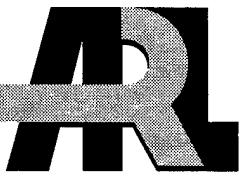


ARMY RESEARCH LABORATORY



Origin of Potential Drops of Bipolar Polymer Electrolyte Membrane Fuel Cells in Constant Current Discharge

Rongzhong Jiang, Charles Walker, and Deryn Chu

ARL-TR-2237

August 2000

Approved for public release; distribution unlimited.

The findings in this report are not to be construed as an official Department of the Army position unless so designated by other authorized documents.

Citation of manufacturer's or trade names does not constitute an official endorsement or approval of the use thereof.

Destroy this report when it is no longer needed. Do not return it to the originator.

Army Research Laboratory

Adelphi, MD 20783-1197

ARL-TR-2237

August 2000

Origin of Potential Drops of Bipolar Polymer Electrolyte Membrane Fuel Cells in Constant Current Discharge

Rongzhong Jiang, Charles Walker, and Deryn Chu

Sensors and Electron Devices Directorate

Sponsored by
U.S. Army Materiel Command
5001 Eisenhower Avenue
Alexandria, VA 22333-0001

Approved for public release; distribution unlimited.

Abstract

Empirical equations were developed to describe the potential-time behaviors of polymer electrolyte membrane fuel cell (PEMFC) stacks at constant current discharge. When either ambient temperature or discharge current is too high, the experimental potential-time curves are inclined or have fallen rapidly within a short discharge time. Various experimental potential-time curves are fitted well with the empirical equations at different discharge current and ambient temperatures. The effect of parameters of the empirical equations on the shape of the potential-time curve is also analyzed. Mass transfer is likely a reason for the rapid falling of the potential, and polymer electrolyte dehydration is responsible for the inclination of the potential-time curves. Empirical equations are helpful for forecasting and explaining the long-term discharge performance of the PEMFC stacks.

Contents

1. Introduction	1
2. Experimental Setup	2
3. Development of Empirical Equations	3
4. Calculated Results	6
4.1 Effect of $T_b - T_o$	6
4.2 Effect of S	6
4.3 Effect of T_m Value	6
4.4 Effect of Parameter A	6
4.5 Effect of Parameter B	7
5. Experimental Results	9
5.1 Temperature-Time Curve	9
5.2 Potential-Time Curves.....	9
6. Conclusions	13
Acknowledgment	14
References	15
Distribution	17
Report Documentation Page	19

Figures

1. Constant current discharge performance of a PEMFC stack at an ambient temperature of 20 °C and at different discharge currents	3
2. Constant current discharge performance of a PEMFC stack at different ambient temperatures	4
3. Calculated curves of stack temperature versus time for a PEMFC stack at a constant current discharge with use of an empirical equation	7
4. Calculated curves of stack voltage versus time for a PEMFC stack at a constant current discharge with use of an empirical equation	8
5. Variation of stack temperature versus time for a PEMFC stack at a constant current discharge and an ambient temperature of 20 °C	9
6. Constant current discharge performance of a PEMFC stack at an ambient temperature of 20 °C.....	10
7. Constant current discharge performance of a PEMFC stack at different ambient temperatures	11
8. Stack voltage dropping with time when either discharge current or ambient temperature was too high for a PEMFC stack at a constant current discharge condition	12

Tables

1. Parameters used for calculations of potential-time curves for a 50-W bipolar PEMFC stack	10
---	----

1. Introduction

For cleaner air and less emitted pollution, fuel cells have been considered one of the most promising innovative energies for electric vehicles and for portable power sources. Among many kinds of fuel cells, polymer electrolyte membrane fuel cells (PEMFCs) have received much attention in the last two decades [1–14] because of their light weight, compactness, high power, and low cost. To understand and improve the performance of PEMFCs, researchers have developed several models [8–13] to explain the behavior of potential variation with the discharge current for single cells and for fuel cell stacks. Kim et al [8] have modeled the potential-current curves for a single fuel cell using an empirical equation, including processes of activation, ohmic, and mass transfer. Amphlett et al [9–10] have tried to describe the relationship of the potential and current of the Ballard Mark IV fuel cell using mechanistic and empirical methods. Chu and Jiang [11–13] have described the potential-current behaviors of PEMFC stacks in the presence of all electrode processes and mass transfer. However, modeling or description of the potential-current behaviors of PEMFCs alone is not enough to know or evaluate the overall performance of fuel cells or fuel cell stacks, because practical fuel cells have to be working for a long time at different ambient temperatures.

During long-term operation of fuel cells, the temperature of a fuel cell stack may change with time. How to assess the effect of temperature and time changes on the performance of fuel cell stacks is a primary consideration when all electrode processes and mass transfer are present. This research is to study the long-term performance of PEMFC stacks at constant current discharge, instead of describing the potential-current behaviors only.

2. Experimental Setup

We used a bipolar PEMFC stack that could provide about 50 W of output power in optimum condition. The open-circuit potential was about 42 V. The active electrode area was about 18 cm^2 , and the volume of the stack was about 250 cm^3 . The stack was humidified with water steam and initially run at 0.5 A for several hours to reach a stable performance before we used it to generate data.

We also used a high purity of hydrogen (99.99%) as fuel and compressed air as oxidant. The ambient temperature was controlled with a Tenney Environment Chamber (model BTRC), which was programmed through a computer with Linktenn II software. An Arbin battery tester (model BT-2043) was used to program and control constant current discharge. A Hewlett-Packard electronic load (model 6050A) and a Hewlett-Packard multimeter were used to measure current and voltage when the stack voltage was greater than 35 V. A Matheson digital flowmeter (LFE 1000H) was used to measure the hydrogen flow. A hydrogen purger was used and set to a 10-s length per 5-min period for all measurements. We adjusted the inlet hydrogen and air pressures to 3 and 5 psi, respectively. An electric fan (about 10 W) was placed toward the stack during stack evaluation for heat dissipation, and a thermocouple was used to measure stack temperature.

3. Development of Empirical Equations

The potential-time curves of PEMFC stacks are not always flat—they sometimes incline slowly or decline rapidly. For example, when the discharge current is too high, the stack potential falls rapidly within a short discharge term. Figure 1 shows the potential-time curves of a 50-W bipolar fuel cell stack at an ambient temperature of 20 °C and at different discharge currents. When the current is 1.0 or 1.5 A, the potential-time curve is only slightly inclined. However, when the current is equal to or higher than 2.0 A, the stack potential falls rapidly within about 35 min of constant current discharge. Figure 2 shows the potential-time curves of a 50-W bipolar fuel cell stack at constant current (1.0 A) discharge and at different ambient temperatures. When the temperature is equal to or higher than 30 °C, the potential-time curve is inclined slowly and then falls rapidly within about 40 min. The origin of the inclined or declined potential-time curves will be explored in this report. Apparently, the discharge potential-time behavior of the PEMFC stack is affected by the variations of stack temperature and discharge time. All the previous models [8–13] were unable to explain or describe this phenomenon. We developed the following equations to solve the problem.

For a fuel cell stack, the stack potential can be described as [11–13]

$$E = E_o - E_{act} - E_{ohmic} - E_{mass}, \quad (1)$$

$$E = E_o - b \log(i) - (R + \Delta R) i - E_{mass}. \quad (2)$$

Figure 1. Constant current discharge performance of a PEMFC stack at an ambient temperature of 20 °C and at different discharge currents.

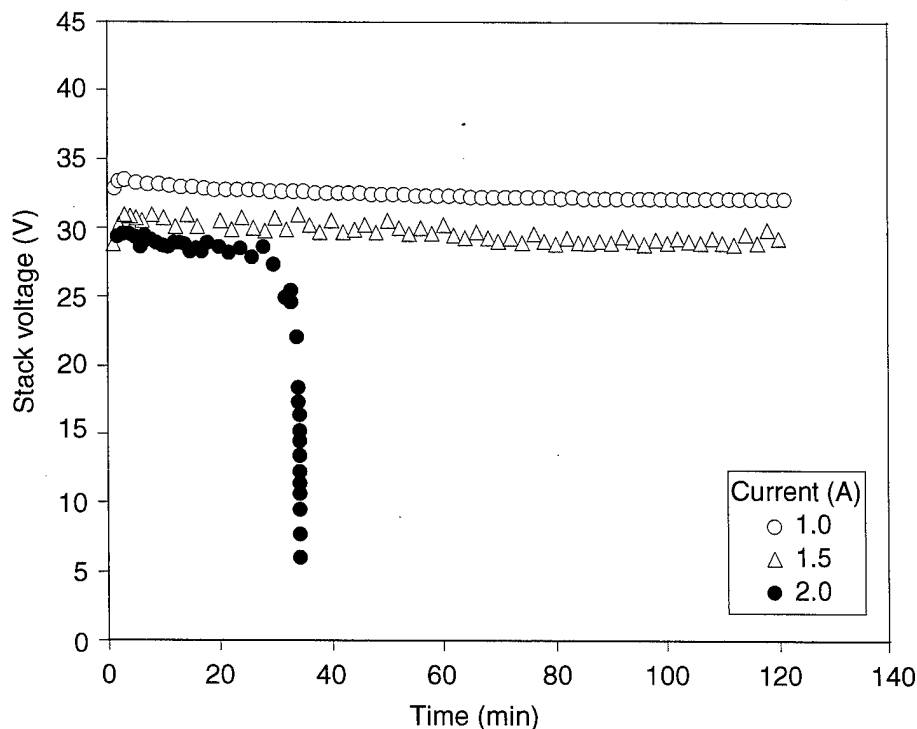
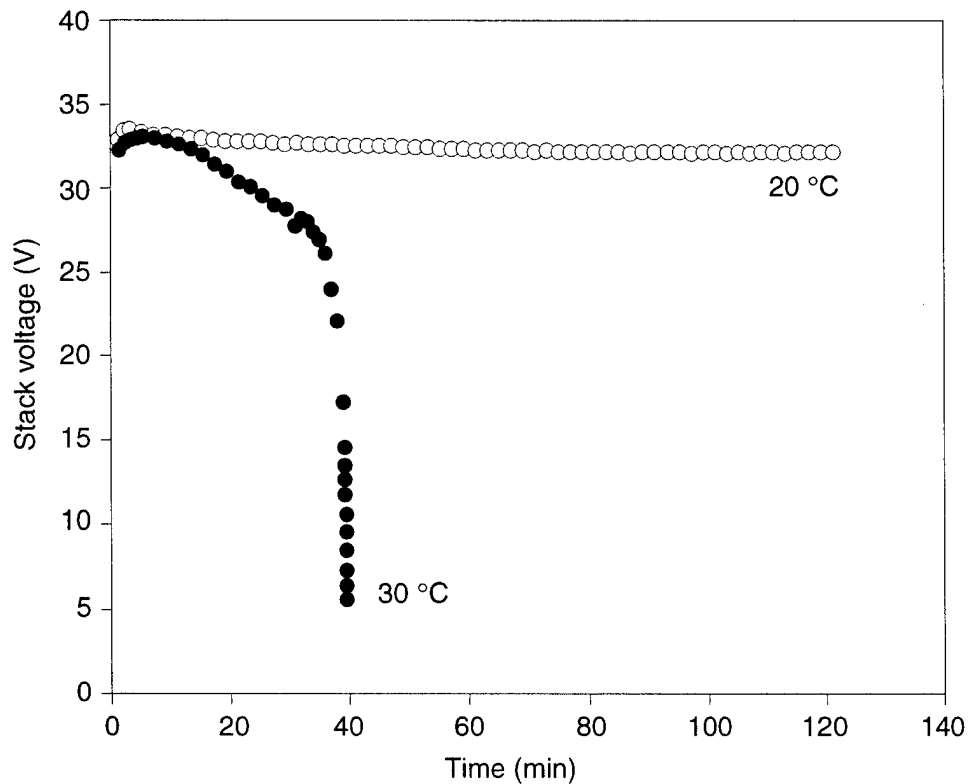


Figure 2. Constant current discharge (1.0 A) performance of a PEMFC stack at different ambient temperatures.



Here, E_o (V) is the open-circuit potential of the stack. E_{ohmic} (V) is the ohmic over potential of the stack, which is equal to the sum of the ohmic over potentials of all single cells linked in a series. E_{mass} (V) is the over potential of the stack caused by mass transfer. The b value is the sum of Tafel slopes of all single cells linked by series, and R is the sum of ohmic resistances of all single cells linked by series. The ΔR is the incremental value of R because of temperature and relative humidity changes.

At constant current discharge, the sum of E_o and activation over potential can be considered a constant if we neglect their variations with temperature. However, the value of R may change appreciably with time, because the effects of stack temperature and polymer electrolyte membrane dehydration on stack ohmic resistance are significant. In addition, the stack temperature may increase with time at constant current discharge until reaching a steady state with the ambient. When stack temperature is too high, the fuel and air transfers may be blocked, interrupted, or unbalanced, causing an appearance of mass transfer over potential. For simplification, equation (2) is rewritten as

$$E = E_a - \Delta R i - E_{\text{mass}} \quad (3)$$

Here, E_a (V) is the apparent potential of the stack at a specific current value, which is equal to the potential at the initial time of constant current discharge. By analyzing a large number of potential-time curves of PEMFC stacks at constant current discharge and at different ambient temperatures and relative humidity, we found that the E_{mass} can be described as

$$E_{\text{mass}} = i A \exp[1/(T_m - T)] \quad (4)$$

Here, A (Ω) is a parameter that affects the rate of stack impedance jump at high temperatures because of mass transfer. T_m ($^{\circ}\text{C}$) is the stack temperature that is high enough to initiate mass-transfer over-potential appearance, and T ($^{\circ}\text{C}$) is the stack temperature at any time.

ΔR can be described as

$$\Delta R = i B \exp[N(T - T_o)/(T_b - T_o)]. \quad (5)$$

Here, B (Ω) is a parameter that affects the rate of ohmic resistance change with stack temperature, N is a function parameter that determines a curvature of selective functions with a different value for each kind of polymer electrolyte stack, T_b ($^{\circ}\text{C}$) is the stack temperature at a steady condition with ambient, and T_o ($^{\circ}\text{C}$) is the ambient temperature.

Therefore, equation (3) can be rewritten as

$$E = E_a - i A \exp[1/(T_m - T)] \pm i B \exp[N(T - T_o)/(T_b - T_o)]. \quad (6)$$

In equation (6), if an increase of stack temperature causes stack resistance to increase, such as polymer electrolyte dehydration at high temperature, the operator on the rightmost side should be minus and vice versa. Moreover, the stack temperature (T) is a function of time. To obtain the potential-time function of the stack, we need to find the stack temperature by experiments. Sometimes, we only know a few points of stack temperature from experiments in a long term of constant current discharge, which is not enough to describe the whole range of stack temperature. Therefore, we need to find a temperature-time function to calculate the other unknown points for the stack.

Unfortunately, stack temperature variation is dependent on many factors, such as stack power, stack size, stack shape, stack-cooling styles, the value of discharge current, and heat dissipation coefficient. It is difficult to obtain an analytical solution. However, an empirical equation to describe the stack temperature-time behavior is obtained for PEMFC stack:

$$T = T_o + (T_b - T_o) t / (t + S), \quad (S > 0). \quad (7)$$

Here, T_o , T_b , and T are described in equation (6), t (min) is discharge time, and S (min) is a time parameter that affects the rate of stack temperature change. At the beginning of discharge, the stack temperature change is the fastest. As time increases, the stack temperature change gradually becomes slower.

With equations (6) and (7), we can calculate the potential-time curves of PEMFC stacks for all electrode processes and mass transfer.

4. Calculated Results

To understand the physical meanings of the parameters described in equations (6) and (7) more clearly, we have performed a series of calculations by varying one parameter only and keeping other parameters constant. These calculated results are summarized in the following sections.

4.1 Effect of $T_b - T_o$

Figure 3(a) shows the calculated data of stack temperature versus time with the use of equation (7), which explain the effect of $T_b - T_o$ on the temperature-time curve at constant current discharge. The stack temperature grows quickly at the beginning of the discharge, especially in the first 20 min. Then the growth slows and the temperature-time curve gradually becomes flat. Through the increase of the value of $T_b - T_o$, the plateau of the temperature-time curve becomes higher.

4.2 Effect of S

Figure 3(b) also shows the calculated data of stack temperature versus time with the use of equation (7), which explain the effect of S on the temperature-time curve at constant current discharge. Through the increase of the value of S , the rate of stack temperature growth decreases, but the plateau of the temperature-time curve changes only a little.

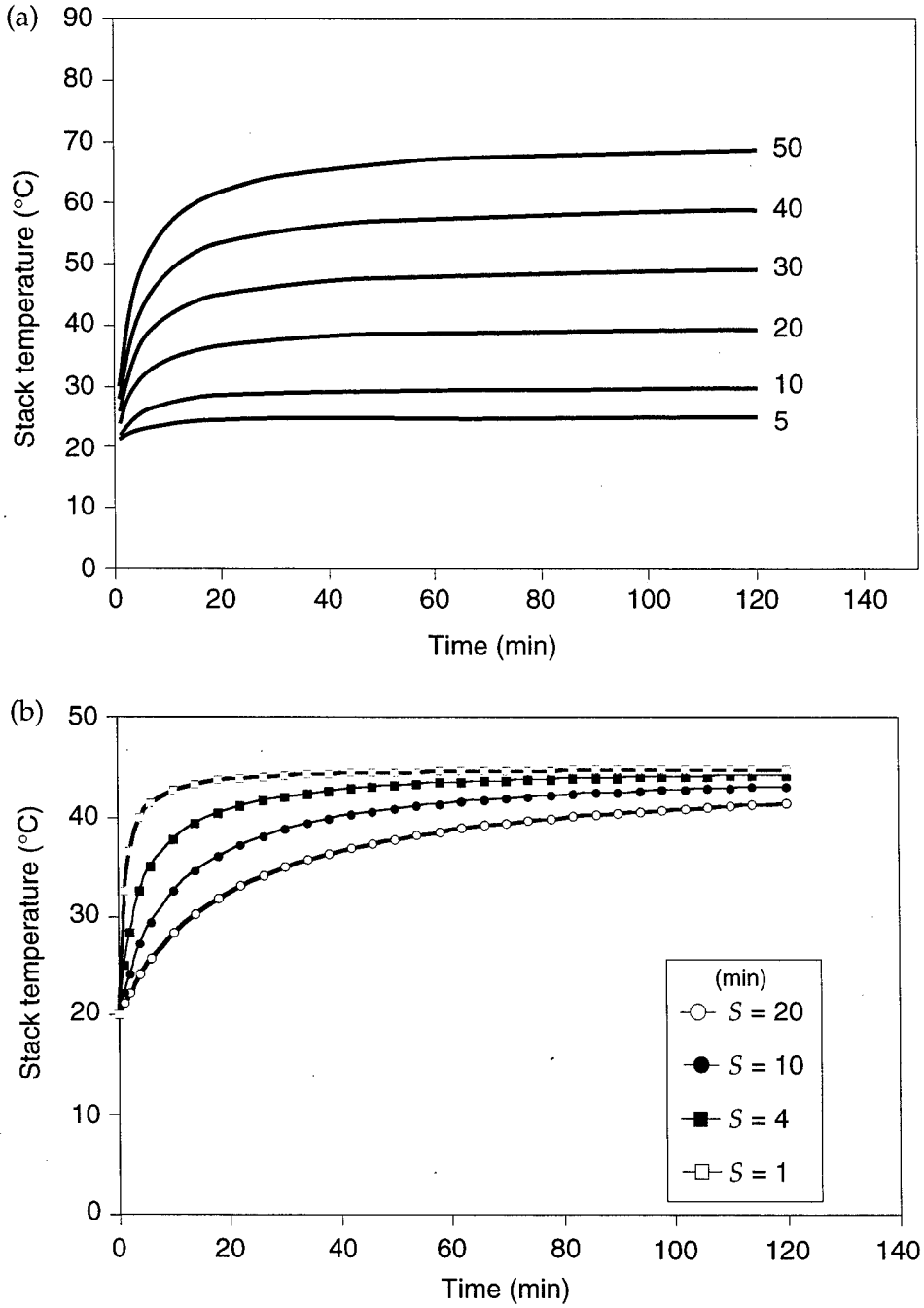
4.3 Effect of T_m Value

Figure 4(a) shows the calculated data of stack voltage versus time, which explain the effect of T_m value on potential-time behavior. With increasing time, the stack temperature gradually reaches the value of T_m and the stack potential begins to decline because of mass-transfer over-potential occurrence. If stack temperature is smaller than the value of T_m , there is no mass-transfer occurrence and no potential falling phenomenon. Because the maximum stack temperature is 43 °C in figure 4(a) (see the top \times curve), the potential-time curve is falling only when the T_m value is equal to or smaller than 43 °C.

4.4 Effect of Parameter A

Figure 4(b) also shows the calculated data of stack voltage versus time, which explain the effect of parameter A on potential-time behavior. With the increase of the value of parameter A , the rate of stack potential declination becomes more significant.

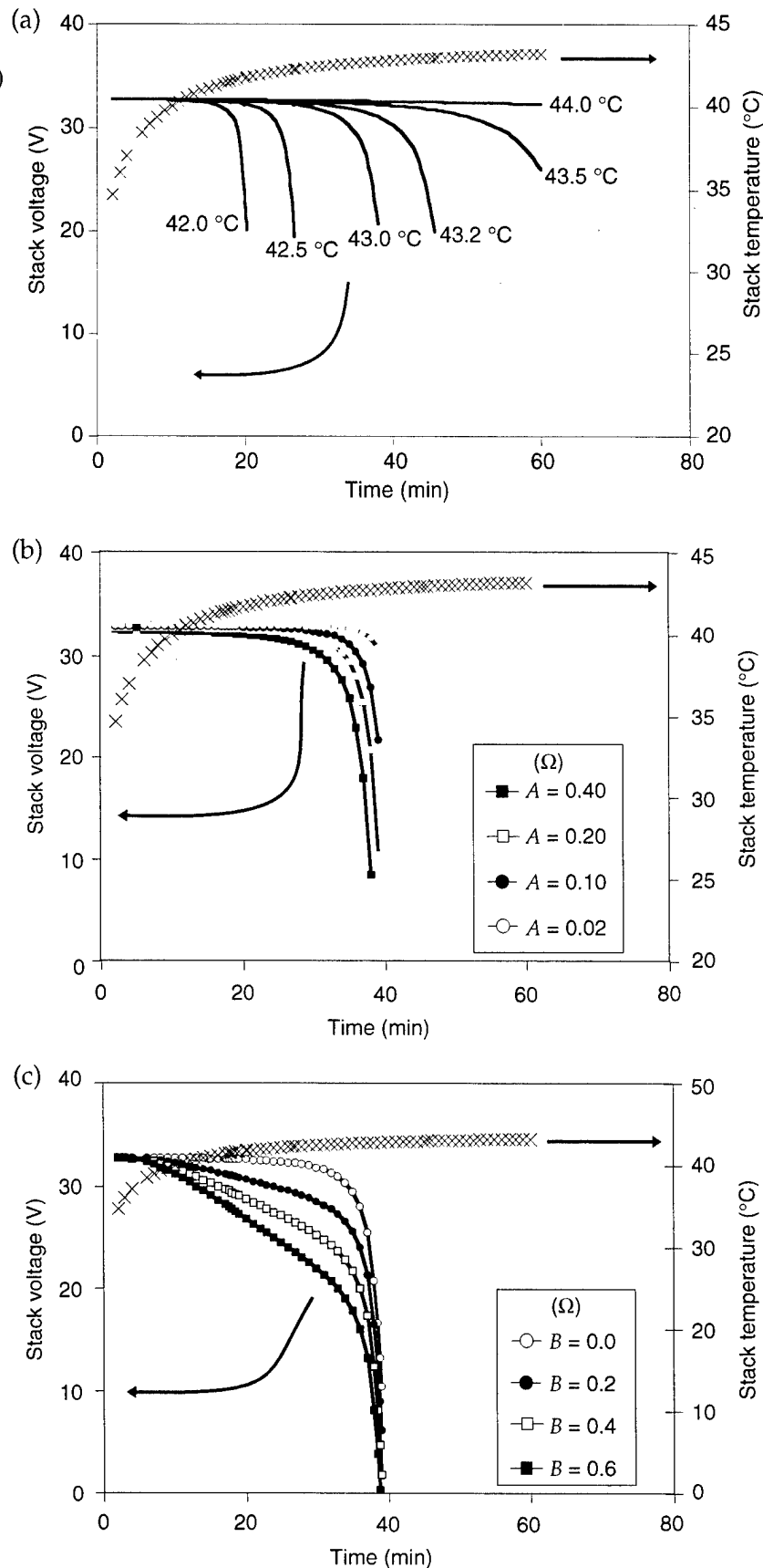
Figure 3. Calculated curves of stack temperature versus time for a PEMFC stack at a constant current discharge with use of an empirical equation. Parameters used:
(a) $T_o = 20^\circ\text{C}$,
 $S = 4.0$ min, and
different $T_b - T_o$
values and
(b) $T_o = 20^\circ\text{C}$,
 $T_b - T_o = 25^\circ\text{C}$, and
different S values.



4.5 Effect of Parameter B

Figure 4(c) also shows the calculated data of stack voltage versus time, which explain the effect of parameter B on the potential-time behavior. Here, the symbol of the term on the rightmost side in equation (6) is considered minus. By increasing the value of parameter B , no apparent effect is shown on the rate of the potential falling. However, the plateau of the potential-time curve becomes more inclined.

Figure 4. Calculated curves of stack voltage versus time (solid lines) for a PEMFC stack at a constant current discharge with use of an empirical equation. Parameters used: (a) $E_a = 33$ V, $A = 0.2 \Omega$, $B = 0$, $i = 1.0$ A, $T_b - T_o = 14.1$ °C, $S = 4.0$ min, $T_o = 30$ °C, and varying T_m values; (b) $E_a = 33$ V, $T_m = 43$ °C, $B = 0$, $i = 1.0$ A, $T_b - T_o = 14.1$ °C, $S = 4.0$ min, $T_o = 30$ °C, and varying A values; and (c) $E_a = 33$ V, $T_m = 43$ °C, $A = 0.2 \Omega$, $i = 1.0$ A, $T_b - T_o = 14.1$ °C, $S = 4.0$ min, $T_o = 30$ °C, $N = 11$, and varying B values. Top line is curve of stack temperature versus time.



5. Experimental Results

5.1 Temperature-Time Curve

By using equation (7), we compare the stack temperatures experimentally recorded with the calculated data. Figure 5 shows the temperature-time curve obtained from a 50-W PEMFC stack at constant current discharge (1.5 A) and at a 20 °C ambient temperature. The points were experimental data, and we calculated the line using equation (7) ($T_o = 20 \text{ }^{\circ}\text{C}$, $T_b - T_o = 19.5 \text{ }^{\circ}\text{C}$, and $S = 4.0 \text{ min}$). As shown in the figure, the calculated curve fits well with the experimental points. In the following calculations for stack potential-time curves, we keep the term S constant (4.0 min) and use different T_o and $T_b - T_o$ values.

5.2 Potential-Time Curves

Effect of Discharge Current: Figure 6 shows a series of potential-time curves at constant current discharge with different current values for a 50-W PEMFC stack. The points and lines were obtained from experiments and calculations, respectively. As shown in the figure, all calculations fit with the experimental points quite well. All the parameters used for the calculations are shown in table 1. With the discharge current increasing, the difference in stack temperature at steady state (T_b) and ambient temperature (T_o) increases, and the stack apparent potential (E_a) decreases. However, the stack temperature that causes mass-transfer over-potential occurrence (T_m) remains unchanged when ambient temperature is kept constant at 20 °C.

Figure 5. Variation of stack temperature versus time for a PEMFC stack at a constant current discharge (1.5 A) and an ambient temperature of 20 °C. Points and line were obtained from experimental and calculated data, respectively. Calculation parameters: $T_o = 20 \text{ }^{\circ}\text{C}$, $T_b - T_o = 19.5 \text{ }^{\circ}\text{C}$, and $S = 4.0 \text{ min}$.

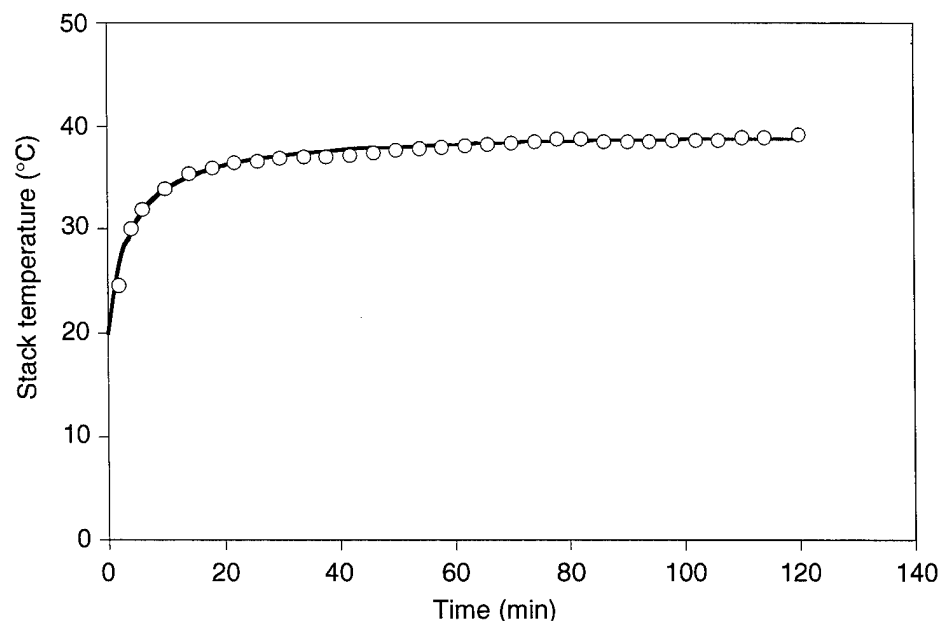


Figure 6. Constant current discharge performance of a PEMFC stack at an ambient temperature of 20 °C. Points and lines were obtained from experimental and calculated data, respectively.

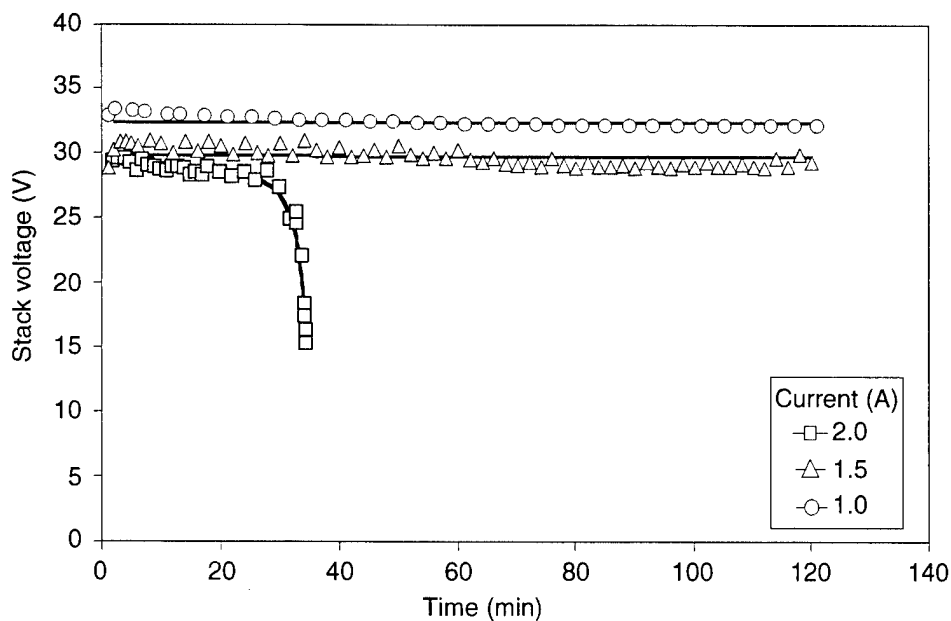


Table 1. Parameters used for calculations of potential-time curves for a 50-W bipolar PEMFC stack.

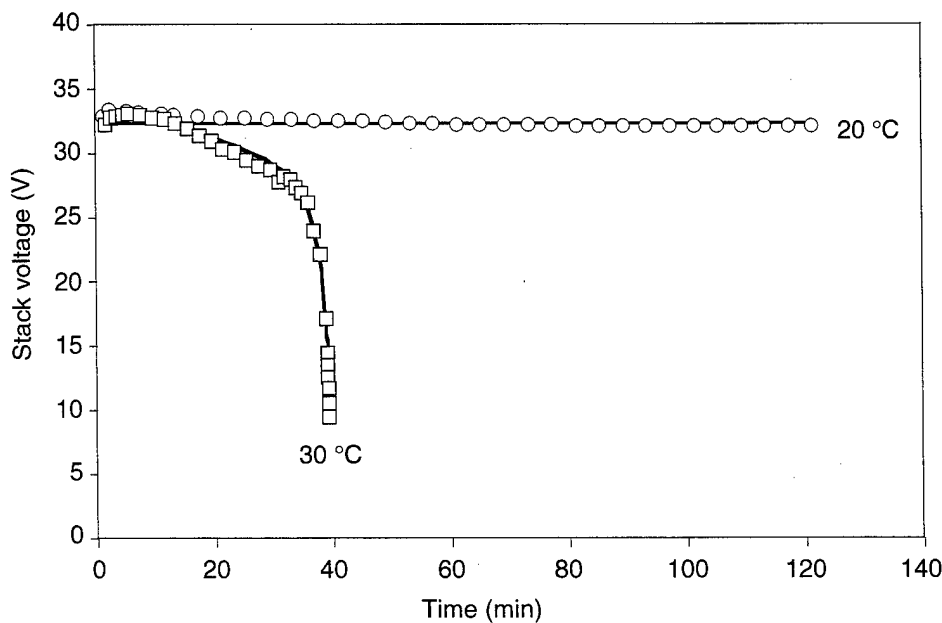
T_o (°C)	I (A)	E_a (V)	A (Ω)	B ($m\Omega$)	T_m (°C)	$T_b - T_o$ (°C)	S (min)
20	1.0	33.0	0.6	0.0	44.0	14.0	4.0
20	1.5	31.0	0.7	0.0	44.0	20.0	4.0
20	2.0	30.0	0.4	0.0	44.0	26.4	4.0
30*	1.0	33.0	0.2	0.2	43.0	14.1	4.0
-5	3.0	24.5	0.1	0.0	38.0	53.6	4.0

*For this calculation, the parameter N equals 11.

Furthermore, at a low value (1.0 A) of constant current discharge, the potential-time curve is relatively flat. Increasing the discharge current value (1.5 A) causes the potential-time curve to become inclined. If the discharge current is too high (2.0 A), the potential-time curve is declined and falls rapidly until reaching zero voltage.

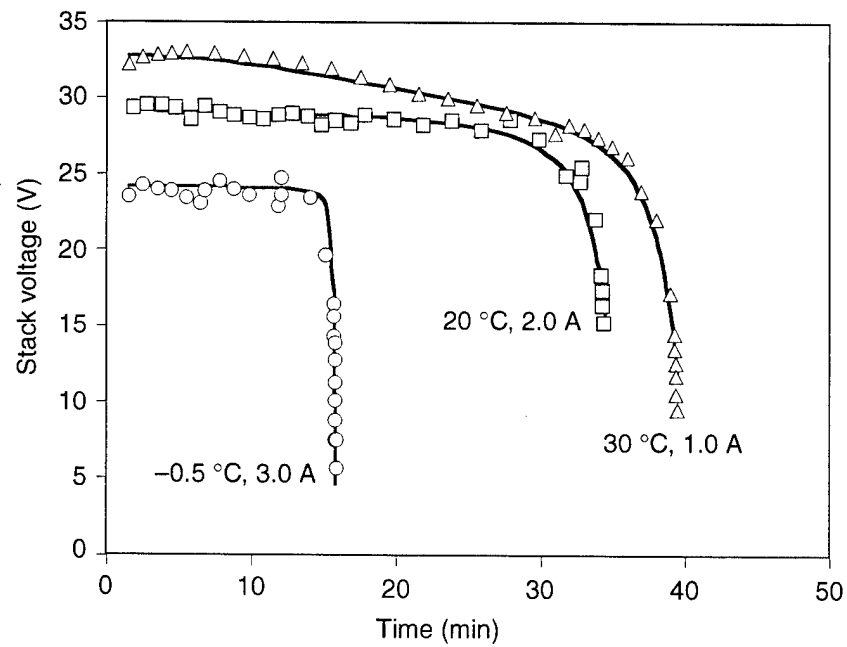
Effect of Ambient Temperature: Figure 7 shows the effect of different ambient temperatures on the potential-time behavior for a 50-W PEMFC stack. The points and lines were obtained from experiments and calculations, respectively. The parameters used for calculations are shown in table 1. With the increase of the ambient temperature from 20 to 30 °C, the values of E_a , T_m , and $T_b - T_o$ do not seem to change significantly. However, the stack T_b value at an ambient temperature of 30 °C is about 10 °C higher than that at an ambient temperature of 20 °C when each has the same value of discharge current (1.0 A). Therefore, at a higher ambient temperature, the stack temperature reaches its T_m value (43 °C) faster. As expected, at $T_o = 20$ °C, the potential-time curve is relatively flat, but at $T_o = 30$ °C, it becomes inclined and falls rapidly to zero voltage within about 40 min. The plateau of potential-time curve is inclined slowly if the parameter B is not zero. Therefore, the parameter B indicates whether the polymer electrolyte membrane is dehydrated.

Figure 7. Constant current discharge (1.0 A) performance of a PEMFC stack at different ambient temperatures. Points and lines were obtained from experimental and calculated data, respectively.



Origin of Potential Declining: Figure 8 shows a series of potential-time curves at constant current discharge for a 50-W PEMFC stack. All these potential-time curves are declined and their potentials fall to zero rapidly within different times. The points and lines in the figure were obtained from experiments and calculations, respectively. As shown in the figure, all calculations fit with the experimental points quite well. All the parameters used for the calculations are shown in table 1. At -5 °C (ambient) and 3.0 A, the discharge current is too high (3.0 A), causing its potential to decline rapidly. At 30 °C (ambient) and 1.0 A, the ambient temperature is too high, causing its potential to fall in a short time. At 20 °C (ambient) and 2.0 A, the potential-time curve is also declined, because of a too-high internal stack temperature caused by a long-term constant current discharge. Therefore, when either ambient temperature or discharge current is too high, which will cause stack internal temperature to increase rapidly, the fuel and air flows may be blocked, interrupted, or unbalanced. Also, a mass-transfer problem may occur and cause a correspondent declination of the potential-time curve in a short time. Besides, when stack internal temperature is too high, the polymer electrolyte membrane may dehydrate, causing an inclination to the plateau of the potential-time curve.

Figure 8. Stack voltage dropping with time when either discharge current or ambient temperature was too high for a PEMFC stack at a constant current discharge condition. Points and lines were obtained from experimental and calculated data, respectively.



6. Conclusions

Several empirical equations are developed to describe the experimental stack temperature-time and the stack potential-time curves for PEMFC stacks at constant current discharge. The experimental stack temperature-time curve fits quite well with equation (7), which contains the parameters of ambient temperature (T_o), stack temperature at a steady state (T_b), and time factor (S). The experimental potential-time curves at different discharge current and ambient temperatures are simulated with equation (6), which contains the parameters of stack internal temperature (T), stack mass-transfer temperature (T_m), and potential decreasing rate factor (A). All these experimental potential-time curves fit quite well with the empirical equations. When stack temperature reaches the value of T_m , a mass-transfer problem occurs, and the potential-time curve is declined rapidly. If either ambient temperature or discharge current is too high, the stack temperature will reach the T_m value and cause a mass-transfer problem. In addition, when the stack internal temperature is too high, the polymer electrolyte membrane will dehydrate, causing an inclination of the potential-time curve.

The empirical equations (6) and (7) are helpful for stack design, because they are likely used for forecasting the stack's long-term performance. We may conduct calculations by setting different parameters for the empirical equations. For example, we may calculate a series of stack temperature-time curves to determine how fast the stack temperature will increase when obtaining a maximum stack power. Also, we may calculate a series of the stack discharge potential-time curves to decide what the stack performance will be, given a specific ambient temperature or discharge current.

Acknowledgment

We wish to thank the U.S. Department of the Army and the Army Materiel Command for their financial support of this project.

References

1. A. J. Apply and E. B. Yeager, "Polymer electrolyte membrane fuel cells," *Energy* **11** (1986), 137.
2. E. A. Ticianelli, C. R. Derouin, and S. Srinivasan, "Localization of platinum in low catalyst loading electrodes to attain high power density in SPE fuel cells," *J. Electroanal. Chem.* **251** (1988), 275.
3. M. S. Wilson and S. Gottesfeld, "Thin-film catalysis layers for polymer electrolyte fuel cell electrodes," *J. Appl. Electrochem.* **22** (1992), 1.
4. H. F. Oetjen, V. M. Schmidt, U. Stimming, and F. Trila, "Performance data of a proton exchange membrane fuel cell using H₂/CO as fuel gas," *J. Electrochem. Soc.* **143** (1996), 3838.
5. M. Uchida, Y. Aoyama, N. Eda, and A. Ohta, "Investigation of the microstructure in the catalyst layer and effects of both perfluorosulfonate ionomer and PTFE-loaded carbon on the catalyst layer of polymer electrolyte fuel cells," *J. Electrochem. Soc.* **142** (1995), 4143.
6. F. N. Buchi, B. Gupta, O. Haas, and G. G. Scherer, "Performance of differently cross-linked, partially fluorinated proton exchange membranes in polymer electrolyte fuel cells," *J. Electrochem. Soc.* **142** (1995), 3044.
7. M. Uchida, Y. Aoyama, N. Eda, and A. Ohta, "New preparation method for polymer-electrolyte fuel cells," *J. Electrochem. Soc.* **142** (1995), 463.
8. J. Kim, S. M. Lee, S. Srinivasan, and C. E. Chamberlin, "Modeling of proton exchange membrane fuel cell performance with an empirical equation," *J. Electrochem. Soc.* **142** (1995), 2670.
9. J. C. Amphlett, R. M. Baumert, R. F. Mann, B. A. Reppley, and P. R. Roberge, "Performance modeling of the Ballard Mark IV solid polymer electrolyte fuel cell, I. Mechanistic model development," *J. Electrochem. Soc.* **142** (1995), 1.
10. J. C. Amphlett, R. M. Baumert, R. F. Mann, B. A. Reppley, and P. R. Roberge, "Performance modeling of the Ballard Mark IV solid polymer electrolyte fuel cell, II. Empirical model development," *J. Electrochem. Soc.* **142** (1995), 9.
11. D. Chu and R. Jiang, "Comparative studies of polymer electrolyte membrane fuel cell (PEMFC) stacks and single cells," *J. Power Sources*, **80** (1999), 226.
12. D. Chu and R. Jiang, "Performance of polymer electrolyte membrane fuel cell (PEMFC) stacks, Part I. Evaluation and simulation of an air-breathing PEMFC stack," *J. Power Sources*, **83** (1999), 128.

-
13. D. Chu, R. Jiang, and C. Walker, "Analysis of PEM fuel cell stacks using an empirical current-voltage equation," *J. App. Electrochem.* **30** (2000), 365.
 14. D. Chu and R. Jiang, "Performance of polymer electrolyte membrane fuel cell stack," *Proc. J. Electrochem. Soc.* **27** (1998), 470.

Distribution

Admnstr Defns Techl Info Ctr Attn DTIC-OCP 8725 John J Kingman Rd Ste 0944 FT Belvoir VA 22060-6218	Commander US Army CECOM Attn AMSEL-RD-CZ-PS-B M Brundage FT Monmouth NJ 07703-5000
Ofc of the Secy of Defns Attn ODDR(E) (R&AT) The Pentagon Washington DC 20301-3080	US Army Info Sys Engrg Cmnd Attn AMSEL-IE-TD F Jenia FT Huachuca AZ 85613-5300
Ofc of the Secy of Defns Attn OUSD(A&T)/ODDR&E(R) R J Trew 3080 Defense Pentagon Washington DC 20301-7100	US Army Materiel Command Attn AMCIO-I-L 7535 Techl Lib 5001 Eisenhower Ave Alexandria VA 22333-0001
Advry Grp on Elect Devices Attn Documents Crystal Sq 4 1745 Jefferson Davis Hwy Ste 500 Arlington VA 22202	US Army Natick RDEC Acting Techl Dir Attn SBCN-T P Brandler Natick MA 01760-5002
AMCOM MRDEC Attn AMSMI-RD W C McCorkle Redstone Arsenal AL 35898-5240	US Army Simulation, Train, & Instrmntn Cmnd Attn J Stahl 12350 Research Parkway Orlando FL 32826-3726
CECOM Night Vsn/Elect Sensors Dircrtr Attn AMSEL-RD-NV-D FT Belvoir VA 22060-5806	US Army Soldier & Biol Chem Cmnd Dir of Rsrch & Techlgry Dircrtr Attn SMCCR-RS I G Resnick Aberdeen Proving Ground MD 21010-5423
Commander CECOM RDEC Attn AMSEL-IM-BM-I-L-R Stinfo Ofc Attn AMSEL-IM-BM-I-L R Hamlen Attn AMSEL-IM-BM-I-L-R Techl Lib Attn AMSEL-RD-AS-BE E Plichta FT Monmouth NJ 07703-5703	US Army Tank-Automtv Cmnd Rsrch, Dev, & Engrg Ctr Attn AMSTA-TR J Chapin Warren MI 48397-5000
Dir for MANPRINT Ofc of the Deputy Chief of Staff for Prsnll Attn J Hiller The Pentagon Rm 2C733 Washington DC 20301-0300	US Army Train & Doctrine Cmnd Battle Lab Integration & Techl Dircrtr Attn ATCD-B J A Klevecz FT Monroe VA 23651-5850
SMC/CZA 2435 Vela Way Ste 1613 El Segundo CA 90245-5500	US Military Academy Mathematical Sci Ctr of Excellence Attn MADN-MATH MAJ R Huber Thayer Hall West Point NY 10996-1786
US Army ARDEC Attn AMSTA-AR-TD M Fisette Bldg 1 Picatinny Arsenal NJ 07806-5000	DARPA Attn S Welby 3701 N Fairfax Dr Arlington VA 22203-1714

Distribution (cont'd)

Nav Rsrch Lab Attn Code 2627 Washington DC 20375-5000	Director US Army Rsrch Ofc Attn AMSRL-RO-D JCI Chang Attn AMSRL-RO-EN B Mann PO Box 12211 Research Triangle Park NC 27709
Nav Surface Warfare Ctr Attn Code B07 J Pennella 17320 Dahlgren Rd Bldg 1470 Rm 1101 Dahlgren VA 22448-5100	US Army Rsrch Lab Attn AMSRL-DD J M Miller Attn AMSRL-CI-AI-R Mail & Records Mgmt Attn AMSRL-CI-AP Techl Pub (3 copies) Attn AMSRL-CI-LL Techl Lib (3 copies)
Marine Corps Liaison Ofc Attn AMSEL-LN-MC FT Monmouth NJ 07703-5033	Attn AMSRL-RO-PS R Paur Attn AMSRL-SE J Pellegrino Attn AMSRL-SE-D E Scannell Attn AMSRL-SE-DC D Chu Attn AMSRL-SE-DC R Jiang Attn AMSRL-SE-DC S Gilman Attn AMSRL-SE-E J Mait Adelphi MD 20783-1197
USAF Rome Lab Tech Attn Corridor W Ste 262 RL SUL 26 Electr Pkwy Bldg 106 Griffiss AFB NY 13441-4514	
AF Wright Aeronautical Labs Attn AFWAL-POOS-2 R Marsh Wright-Patterson AFB OH 45433	
Hicks & Associates Inc Attn G Singley III 1710 Goodrich Dr Ste 1300 McLean VA 22102	
Palisades Inst for Rsrch Svc Inc Attn E Carr 1745 Jefferson Davis Hwy Ste 500 Arlington VA 22202-3402	

REPORT DOCUMENTATION PAGE			<i>Form Approved OMB No. 0704-0188</i>
<p>Public reporting burden for this collection of information is estimated to average 1 hour per response, including the time for reviewing instructions, searching existing data sources, gathering and maintaining the data needed, and completing and reviewing the collection of information. Send comments regarding this burden estimate or any other aspect of this collection of information, including suggestions for reducing this burden, to Washington Headquarters Services, Directorate for Information Operations and Reports, 1215 Jefferson Davis Highway, Suite 1204, Arlington, VA 22202-4302, and to the Office of Management and Budget, Paperwork Reduction Project (0704-0188), Washington, DC 20503.</p>			
1. AGENCY USE ONLY <i>(Leave blank)</i>	2. REPORT DATE August 2000	3. REPORT TYPE AND DATES COVERED Progress, Oct 1998 to Sept 1999	
4. TITLE AND SUBTITLE Origin of Potential Drops of Bipolar Polymer Electrolyte Membrane Fuel Cells in Constant Current Discharge			5. FUNDING NUMBERS DA PR: N/A PE: 62120A
6. AUTHOR(S) Rongzhong Jiang, Charles Walker, and Deryn Chu			
7. PERFORMING ORGANIZATION NAME(S) AND ADDRESS(ES) U.S. Army Research Laboratory Attn: AMSRL-SE-DC 2800 Powder Mill Road Adelphi, MD 20783-1197			8. PERFORMING ORGANIZATION REPORT NUMBER ARL-TR-2237
9. SPONSORING/MONITORING AGENCY NAME(S) AND ADDRESS(ES) U.S. Army Materiel Command 5001 Eisenhower Avenue Alexandria, VA 22333-0001			10. SPONSORING/MONITORING AGENCY REPORT NUMBER
11. SUPPLEMENTARY NOTES ARL PR: 9NV4VV AMS code: 622120.H16			
12a. DISTRIBUTION/AVAILABILITY STATEMENT Approved for public release; distribution unlimited.		12b. DISTRIBUTION CODE	
13. ABSTRACT <i>(Maximum 200 words)</i> Empirical equations were developed to describe the potential-time behaviors of polymer electrolyte membrane fuel cell (PEMFC) stacks at constant current discharge. When either ambient temperature or discharge current is too high, the experimental potential-time curves are inclined or have fallen rapidly within a short discharge time. Various experimental potential-time curves are fitted well with the empirical equations at different discharge current and ambient temperatures. The effect of parameters of the empirical equations on the shape of the potential-time curve is also analyzed. Mass transfer is likely a reason for the rapid falling of the potential, and polymer electrolyte dehydration is responsible for the inclination of the potential-time curves. Empirical equations are helpful for forecasting and explaining the long-term discharge performance of the PEMFC stacks.			
14. SUBJECT TERMS Fuel cell stack, discharge performance, PEMFC, fuel cell modeling		15. NUMBER OF PAGES 25	16. PRICE CODE
17. SECURITY CLASSIFICATION OF REPORT Unclassified	18. SECURITY CLASSIFICATION OF THIS PAGE Unclassified	19. SECURITY CLASSIFICATION OF ABSTRACT Unclassified	20. LIMITATION OF ABSTRACT UL